Broadband Characterization of High-Dielectric Constant Films for Power-Ground Decoupling

Jan Obrzut, *Member, IEEE*, Natsuko Noda, and Ryusuke Nozaki

Abstract—We evaluated the broadband dielectric permittivity and impedance characteristics of high dielectric constant films for decoupling capacitance applications at frequencies of 100 to 10 GHz. In order to extend the measurements to the microwave range, we developed an appropriate expression for the input admittance of a thin-film capacitance terminating a coaxial line. The theoretical model treats the capacitance as a distributed network and correlates the network scattering parameter with complex permittivity of the specimen. The method eliminates the systematic uncertainties of the lumped element approximations and is suitable for high-frequency characterization of low-impedance substrates.

Index Terms—Broadband measurements, coaxial discontinuity, decoupling capacitance, dielectric permittivity, microwave characterization, TDR.

I. INTRODUCTION

THE NEED for power-ground decoupling is nearly universal in electronic circuits in order to secure signal integrity and reduce electromagnetic interference noise. Current technologies utilize surface-mounted discrete chip-capacitors, which become ineffective when the operating frequency increases above several hundred megahertz [1]. High-dielectric constant (high-k) polymer-ferroelectric ceramic composites that exhibit certain high-frequency loss have recently shown promise for embedded decoupling capacitance (EDC) and power planes with desirable, low-impedance characteristics over a broad frequency range, including the microwave [1]. Advancing EDC technology requires a suitable test method to measure the material dielectric properties and to assess the impedance characteristic in planar, thin-film configuration over a broad frequency range. A broadband measurement method of complex permittivity in the coaxial configuration was proposed for bilayered materials. Higher order TM-type evanescent modes excited at the coaxial discontinuity were analyzed by the mode-matching method [2]. This model, however, is not applicable to single nonconducting films. Such films have been typically evaluated using a lumped element approximation. The existing broadband lumped element methods assume

quasistatic conditions in the thin-film specimen [3]. They fail to produce meaningful results at frequencies above a few hundred megahertz [4], especially in the case of high-dielectric constant films.

In this paper, we describe a broadband measurement methodology which is based on observation and analysis of the fundamental mode in a film specimen terminating a coaxial transmission line. Using this test technique, the dielectric permittivity and impedance of several industry-developed high-dielectric constant films were accurately evaluated at frequencies of 100 to 10 GHz.

II. THEORETICAL ANALYSIS

The experimental arrangement under consideration is shown in Fig. 1. A dielectric disk specimen of thickness d and the relative complex permittivity $\varepsilon^* = \varepsilon' - j\varepsilon''$ is placed at the end of the center conductor of a coaxial airline. The diameter of the specimen, a, matches that of the center conductor. The specimen is covered with the counter conductor and forms a circular parallel-plate capacitor. Such structures are assumed to satisfy the lumped element approximation if the length of the propagating wave is much longer than the film thickness [5]. Since the specimen is short terminated, the wave should be reflected back after a time delay of $\tau \approx 2d\sqrt{\varepsilon'}/c$. In the case of a circular film specimen with a diameter of 3.0 mm, thickness of 100 μm and ε' of about 38, this double-passing time delay would have been approximately 4 ps. The time delay measured for such a specimen in a TDR experiment is in the range of about 60 ps, which is consistent with $\tau \approx a\sqrt{\varepsilon'}/c$, indicating dependence on the diameter of the specimen rather than on its thickness [6]. The structure in Fig. 1 can be therefore electrically equivalent to a network, where the dielectric film represents a transmission line inserted between two matched transmission lines. Consequently, the scattering coefficient S_{11}, resulting from the combination of the wave multiple reflection and transmission components in the specimen section, can be expressed by the following equation [7]:

$$S_{11} = \rho + \sum_{n=1}^{\infty} (-\rho e^{-\gamma a})^{n-1}(1-\rho^2)e^{-\gamma a} = \frac{\rho + e^{-\gamma a}}{1 + \rho e^{-\gamma a}} \quad (1)$$

where ρ is the complex reflection coefficient for nonmagnetic media; $\rho = (1-\sqrt{\varepsilon^*})/(1+\sqrt{\varepsilon^*})$; γ is the propagation constant, $\gamma = j\omega/c\sqrt{\varepsilon^*}$; ω is an angular frequency; and c is the speed of light in air. The input admittance of the specimen section Y_{in}, having characteristic conductance of G_s, can be expressed in

terms of the circuit parameters where the specimen represents an unmatched termination whose reflection coefficient is Γ

$$Y_{in} = G_s \frac{1 - \Gamma}{1 + \Gamma}. \tag{2}$$

Since a matched load follows the termination, the scattering coefficient of the network S_{11} equals Γ. Combining (1) with (2) leads to (3)

$$Y_{in} = G_s \frac{(1 - \rho)(1 - e^{-\gamma a})}{(1 + \rho)(1 + e^{-\gamma a})}. \tag{3}$$

Introducing $x = (\omega a/2c)\sqrt{\varepsilon^*}$, (3) can be expressed as

$$Y_{in} = G_s \frac{j\omega a}{2c} \varepsilon^* \frac{1}{x \cot(x)}. \tag{4}$$

The specimen section in (4) represents a transmission line having an electrical length of $a/2$. In the complex capacitance notation, the characteristic conductance per unit of length represents the geometric capacitance C_p of the empty specimen section, $C^* = G_s (a/2c) \varepsilon^* = C_p \varepsilon^*$. The term $1/x \cot(x)$ accounts for the wave propagation in the specimen. If the electrical length is small in comparison to the wavelength, $a \ll \lambda$, $x \ll 1$, the value of the $x \cot(x)$ approaches unity and (4) simplifies to the conventional expression for the input admittance of a transmission line terminated with a lumped shunt capacitance [5].

During measurements, the reference plane is set at the interface between the end of the coaxial line having the characteristic conductance G_l and the dielectric specimen section with the characteristic conductance G_s. According to [5] and [8], a cell constant parameter G_s/G_l can be determined by evaluating the fringing field capacitance C_f around the specimen section. Using the fringing field capacitance and equation (4), we finally arrive at (5) for the complex permittivity of the film specimen

$$\varepsilon^* = \frac{G_l}{j\omega C_p} \frac{1 - S_{11}^m}{1 + S_{11}^m} \cdot x \cot(x) - \frac{C_f}{C_p} \tag{5}$$

where S_{11}^m is the measured scattering coefficient of the network. At sufficiently low frequencies, $x \cot(x)$ approaches the value of one and (5) simplifies to the conventional lumped element model [3], which can be used for initial estimation in iterative solution of (5).

III. EXPERIMENTAL

An experimental coaxial test fixture was constructed from two APC-7 mm to APC-3.5 mm microwave adapters. The center conductor was replaced with a fixed 3.0 mm diameter pin, machined precisely to achieve flat and parallel contact between the film specimen and the APC-7 mm short termination. High-dielectric constant EDC films, EDC1-4 (Epoxy resins ferroelectric ceramics composites) and EDC5 (Polyimide ferroelectric ceramic composite), were obtained from the NCMS Embedded Capacitance Project [1]. The dielectric properties determined for these materials using a microstrip resonator technique are listed in Table I. The circular film specimens with a 3.0 mm diameter for broadband measurements were defined by photolithography.
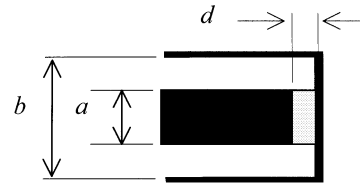

Fig. 1.   Diagram of the test fixture.

The time-domain reflectometry (TDR) measurements were carried out using a Tektronix 11 802 Digital Sampling Oscilloscope equipped with a TEK SD-24 TDR/Sampling Head. Waveforms were captured in a 10 ns window typically containing 1024 data points with a resolution of 2.5 ps. The relative combined standard uncertainty of the impedance determined by TDR was about 5%. The measurements in the frequency domain were carried out using a network analyzer (HP 8720D) in the frequency range between 100 MHz and 10 GHz. One-port open, short, and broadband load calibration was performed using an HP 85050B APC-7 calibration kit. The relative combined standard uncertainty in geometrical capacitance measurements was 2%. The largest contributing factor to the uncertainty was the uncertainty in the film thickness measurements of 1 μm. The relative standard uncertainty of S_{11}^m was assumed to be within the manufacturer's specification for the HP 8720D. The combined relative experimental uncertainty in complex permittivity was within 8%, while the experimental resolution of the dielectric loss tangent measurements was about 0.01.

IV. RESULTS AND DISCUSSION

Fig. 2 shows the TDR response reflected at the EDC films in the coaxial test fixture (Fig. 1). The measurements are normalized to the 50 Ω impedance of a precision coaxial air-filled transmission line. It is seen that at the time delay τ_o (or at highest frequencies ω) all the EDC specimens show the lowest impedance as expected for a capacitive load. At longer lengths of time, the voltage builds up across the complex capacitance $C_p \varepsilon^*$, increasing its impedance until it effectively becomes an open circuit. An inductive delay, which is a common source of error in impedance measurements, does not visibly contribute to the measured response. From the viewpoint of power-ground decoupling, the test capacitor can source the charge as long as its impedance is lower than the reference input impedance. The best performance is qualitatively indicated by the response close to that of zero impedance (short) termination, which is shown in Fig. 2(b) for film EDC4, followed by EDC3 [(Fig. 2(c)], EDC5 [Fig. 2(d)], and film EDC2 [Fig. 2(e)]. The impedance increases with decreasing capacitance density. In comparison to other EDC materials tested, the EDC4 had the highest capacitance density of about 2.5_nF/cm^2, while EDC2 showed the lowest capacitance density of about 0.07 nF/cm^2. (Table I). For a given geometric capacitance, lower impedance will result from a dielectric material with higher complex permittivity ε^*.

The quantitative analysis of the impedance characteristics was performed in the frequency domain. An example of the frequency-dependent impedance determined directly from

TABLE I
DIELECTRIC CONSTANT, ε', LOSS TANGENT, tan (δ), AND CAPACITANCE DENSITY, C_A OF THE EDC FILMS OF THICKNESS d, MEASURED ON MICROSTRIP RESONATORS AT THE RESONANT FREQUENCY f_r

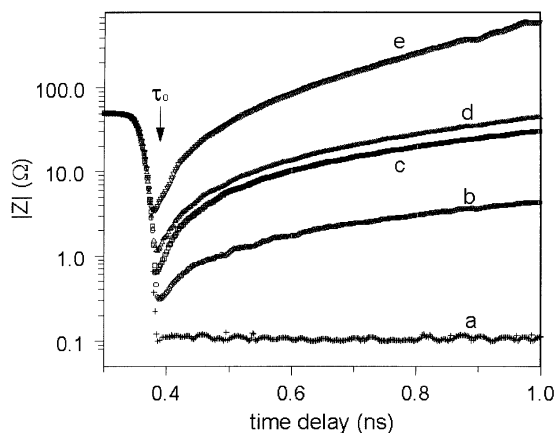| Material	d (μm)	f_r (GHz)	ε'	tan (δ)	C_A (nF/cm^2)
EDC1	80	0.889	34.6	0.05	0.38
EDC2	50	0.928	3.88	0.02	0.07
EDC3	100	0.842	38.6	0.03	0.34
EDC4	8	1.112	22.1	0.08	2.5
EDC5	48	1.093	11.8	0.01	0.25

Fig. 2. Impedance characteristics of the EDC films determined from the TDR waves, (a) short termination, (b) EDC4 (c) EDC3, (d) EDC5, and (e) EDC2.
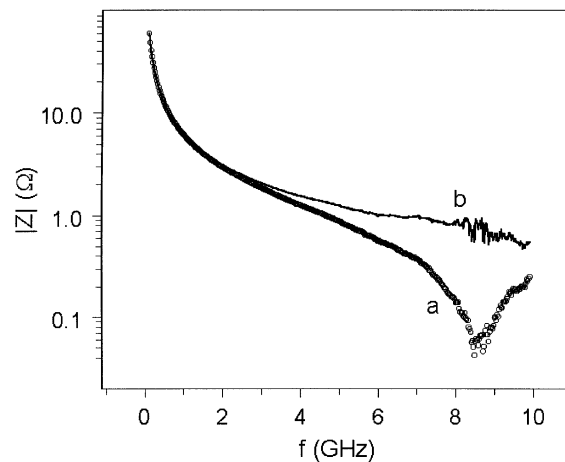

Fig. 3. Broadband impedance of EDC1 films, (a) determined directly from a single port reflection measurement, (b) corrected for the wave propagation in the specimen section.

one-port reflection measurements is shown in Fig. 3(a) for the EDC1 films having permittivity of 34.6–j1.6. The measurements are normalized to the 50 Ω impedance of a precision coaxial air-filled transmission line. At about 8.2 GHz, there is a noticeable dip of about 0.02 Ω in the impedance, due to resonant absorption that leads to systematic uncertainties as the frequency increases above 2 GHz. The application of the propagation model eliminates these difficulties. Correcting the measured impedance Z_m using the wave propagation term $Z_{corr} = Z_m/x \cot(x)$ leads to the results shown in Fig. 3b, which properly reflect the electrical characteristic of a capacitance load. The corrected impedance decreases with increasing frequency, reaching the value of about 0.8 Ω at 8.4 GHz, which is over an order of magnitude higher than that determined from the direct reflection measurements.

It appears that the coaxial test fixture configuration and the propagation model allow for an accurate determination of impedance, which can satisfy the requirements involved in characterization of thin dielectric films and low-impedance substrates for the decoupling capacitance functions. Undesired oscillation of impedance at resonant and clock frequencies in real circuits can be conveniently suppressed by tailoring the dielectric loss mechanism of the EDC material.

Measurements of the dielectric constant ε' and the dielectric loss ε'', are illustrated in Fig. 4(a) and (b) for EDC3 films. The results obtained from the lumped element model (7) are also plotted for comparison in Fig. 4(c) and (d), respectively. The ε' of EDC3 decreases from about 40 at 100 MHz to about 38

at 5 GHz, while the dielectric loss [Fig. 4(b)] increases from about 0.4 to 1.8 with increasing frequency. The permittivity results obtained for the EDC films agree well with the microstrip resonance data (Table I) where the differences are within 1% for ε' and 4% for ε''. The experimental results indicate that (5) correctly describes the complex permittivity of the EDC films over a broad frequency range. In contrast, application of the lumped element model results in an abnormal increase in both ε', and ε'' as frequency increases, leading to systematic errors, which at higher frequencies considerably exceed the combined experimental uncertainty. The relative systematic uncertainty of the lumped element method for permittivity $\Delta \varepsilon_s^*$ may be obtained from (5), $\Delta \varepsilon_s^* = 1/x \cot(x) - 1$. The term describing the propagation effect in (4) and (5), $x \cot(x)$, has a singularity when $x = \pi/2$, which corresponds to a half-wavelength resonance at frequency $f_r = c/2a\sqrt{\varepsilon^*}$. The resonant frequency depends on the diameter of the specimen and its permittivity. In the case of loss-less dielectrics, the parameter x is real, and the $\Delta \varepsilon_s^*$ function oscillates singularly between $\pm\infty$, near the resonant frequency. For film samples with finite dielectric loss, the real part of $\Delta \varepsilon_s^*$ undergoes an oscillation, reaching zero at the resonant frequency, while the imaginary part shows a peak value at the resonant frequency. Consequently, the abnormal increase in permittivity, observed at higher frequencies for the film samples treated as a lumped element, can be attributed to the tails of the resonant absorption. Fig. 3 shows that the experimental data are somewhat distorted near f_r. The distortion may originate from excitation of higher order modes due to imperfection in the geometry of the test fixture, which, in practice, limits the applicability of the testing at frequencies higher than 0.8 f_r. Nevertheless, the basic feature of the experimental data obtained for EDC films is essentially the same as that predicted by the $x \cot(x)$, which provides further support for the utilization of the presented approach.

V. CONCLUSION

Complex permittivity and impedance characteristics of high-k dielectric films for embedded decoupling capacitance can be accurately evaluated in a broad frequency range, using
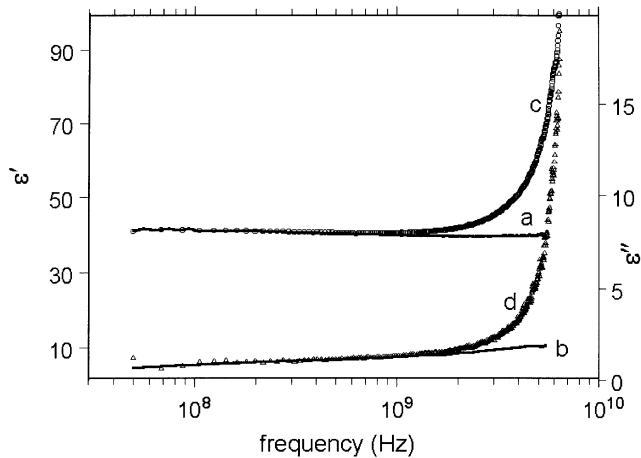
Fig. 4.   Dielectric permittivity of EDC3 films: (a) dielectric constant, (b) dielectric loss; (c) and (d) dielectric constant and dielectric loss determined according to the lumped capacitance model.

the propagation model for thin-film capacitance terminating a coaxial transmission line. The specimen section represents a transmission line having an electrical length of $a/2$. At low frequencies, where the electrical length is small in comparison to the wavelength, the propagation model simplifies to the conventional expression for the input admittance of a transmission line terminated with a lumped shunt capacitance. At higher frequencies, the presented testing methodology eliminates systematic uncertainties of the lumped element approximations and allows for accurate impedance measurements at frequencies of up to 0.8 f_r. The resonant frequency, f_r, depends on the diameter of the specimen and its permittivity. In the frequency range of 100 MHz to about 10 GHz, the electrical characteristic of high-k films was found to be consistent with a capacitance load, without noticeable contribution from the circuit inductance that typically causes a series resonance and obscures the high-frequency response.

REFERENCES

[1] T. Hubbing and M. Xu, "Electronic design considerations for printed circuit boards with embedded capacitance," NCMS, 3025 Boardwalk, Ann Arbor, MI 48 108, NCMS Embedded Capacitance Project Rep. 0091RE00, Dec. 2000.
[2] N. Beldhadj-Tahar, O. Mayer, and A. Fourrier-Lamer, "Broad-band microwave characterization of bi-layerd materials using a coaxial discontinuity with applications for thin conductive films for microelectronics and material in air-tight cell," *IEEE Trans. Microwave Theory Tech.*, vol. 45, pp. 260–267, 1997.
[3] M. A. Stuchly and S. S. Stuchly, "Coaxial line reflection methods for measuring dielectric properties of biological substances at radio and microwave frequencies: A review," *IEEE Trans. Instrum. Meas.*, vol. IM–29, pp. 176–183, 1980.
[4] F. I. Mopsik, "Extended frequency range dielectric measurements of thin films," *Rev. Sci. Instrum.*, vol. 71, pp. 2456–2460, 2000.
[5] N. Marcuvitz, *Waveguide Handbook*.   New York: McGraw-Hill, 1951.
[6] J. Obrzut and R. Nozaki, "Permittivity measurements of high dielectric constant films at microwave frequencies," in *IPC Tech. Conf. Proc. S08*, San Diego, CA, April 1–5, 2000, pp. 61–63.
[7] R. Nozaki and J. Obrzut, "Broadband complex permittivity measurements of solid films at microwave frequencies," unpublished.
[8] M. F. Iskander and S. S. Stuchly, "Fringing field effect in the lumped-capacitance method for permittivity measurements," *IEEE Trans. Instrum. Meas.*, vol. IM–27, pp. 107–109, 1978.

Jan Obrzut (M'00) received the Ph.D. degree in technical sciences from the Institute of Physics, Cracov Polytechnic, Poland, in 1981.

After a postdoctoral appointment at the Polymer Science Department, University of Massachusetts, Amherst, he was a researcher at the Five College Radio Astronomy Department, Amherst, working on microwave dielectric waveguides. He joined IBM in 1988 as Advisory Engineer, where he was conducting exploratory work on the application of polymer dielectrics in microelectronics. He has been with the NIST Polymers Division since 1997, where he does research in metrology of dielectric films and hybrid materials for microwave and electronic applications. His research interests include molecular dynamics and interfacial interactions in polymers, blends, and nanocomposites.

Dr. Obrzut is a member of the American Physical Society.

Natsuko Noda received the Ph.D. degree in experimental physics from Hokkaido University, Sapporo, Japan, in 2000.

She is currently a Guest Researcher at National Institute of Standards and Technology, Gaithersburg, MD. Her research interests include broadband dielectric relaxation spectroscopy and dielectric properties of polymers and polymer composites filled with ferroelectric ceramics.

Ryusuke Nozaki was born in Tokyo, Japan, in 1957. He received the B.S. and the M.S. degrees in physics from Tokai University, Kanagawa, Japan, in 1982 and 1984, respectively, and the Ph.D. degree in physics from Waseda University, Tokyo, Japan, in 1987.

In 1985, he joined the Department of Applied Physics, Waseda University. From 1988 to 1992, he worked with the Dielectric Research Group, Universite du Quebec a Trois-Rivieres, QC, Canada. In 1992, he joined the Department of Physics, Hokkaido University, Hokkaido, Japan. Since 1995, he has been with the Division of Physics, Graduate School of Science, Hokkaido University. From 1999 to 2000, he was with the National Institute of Standards and Technology, Gaithersburg, MD, as a Guest Researcher. His interests include dielectric relaxation processes in complex systems such as glass-forming fluids, bio-materials, liquid crystals, and aqueous solutions.